ISSN 1063-7761, Journal of Experimental and Theoretical Physics, 2020, Vol. 131, No. 6, pp. 940–944. © Pleiades Publishing, Inc., 2020.
Russian Text © The Author(s), 2020, published in Zhurnal Eksperimental'noi i Teoreticheskoi Fiziki, 2020, Vol. 158, No. 6, pp. 1083–1088.

Atomic and Electronic Structure of SiO_x Films Obtained with Hydrogen Electron Cyclotron Resonance Plasma

T. V. Perevalov[a,b,*], R. M. Kh. Iskhakzai[a], V. Sh. Aliev[a], V. A. Gritsenko[a,b], and I. P. Prosvirin[c]

[a] *Rzhanov Institute of Semiconductor Physics, Russian Academy of Sciences, Siberian Branch, pr. Akademika Lavrentyeva 13, Novosibirsk, 630090 Russia*

[b] *Novosibirsk State University, ul. Pirogova 2, Novosibirsk, 630090 Russia*

[c] *Boreskov Institute of Catalysis, Russian Academy of Sciences, Siberian Branch, pr. Akademika Lavrentyeva 5, Novosibirsk, 630090 Russia*

***** *E-mail: timson@isp.nsc.ru*

Received May 7, 2020; revised June 30, 2020; accepted July 1, 2020

Abstract—The silicon oxide thin films obtained by thermal SiO_2 treatment in hydrogen electron cyclotron resonance plasma at various exposure times are investigated. Using X-ray photoelectron spectroscopy, we have established that such treatment leads to a significant oxygen depletion of thermal SiO_2, the more so the longer the treatment time. The atomic structure of the $SiO_{x<2}$ films obtained in this way is described by the random bonding model. The presence of oxygen vacancies in the plasma-treated films is confirmed by comparing the experimental valence band photoelectron spectra and those calculated from first principles, which allows the parameter x to be estimated. We show that thermal silicon oxide films treated in hydrogen plasma can be successfully used as a storage medium for a nonvolatile resistive memory cell.

DOI: 10.1134/S1063776120110084

1. INTRODUCTION

Oxygen-depleted silicon oxide ($SiO_{x<2}$) films are a promising candidate for the active medium of resistive memory elements (memristors), whose principle of operation is based on the reversible switching of the oxide layer in a metal–insulator–metal (MIM) structure between the high and low resistance states (resistive random access memory, RRAM) [1, 2]. The resistive states in memristors based on silicon oxide are believed to be switched through the electrodiffusion of oxygen vacancies in the insulating layer that leads to the formation/breaking of a conducting filament [3, 4]. The advantage of SiO_x over other insulators suitable for use as an active RRAM medium is its compatibility with the standard technological processes of modern microelectronics.

At present, the technologies for the synthesis of thin stoichiometric oxide films have been well developed. One promising method of obtaining nonstoichiometric oxygen-depleted films is the treatment of a stoichiometric oxide in hydrogen electron cyclotron resonance (ECR) plasma. The merit of the hydrogen ECR plasma is a high degree of ionization at a relatively low ion temperature and a low burning pressure (up to 10^{-3} Pa), so that the thermal effect on the film surface is small during its treatment. This method proved to be good during partial V_2O_5 reduction [5]. In addition, it was established that the treatment of HfO_2 films in hydrogen plasma leads to their oxygen depletion (the formation of $HfO_{x<2}$) and an improvement of the storage characteristics of memristors based on this oxide [6]. Using a nonstoichiometric oxide as the active layer of a memristor is interesting, in particular, as a way of solving the forming problem, which necessitates a high voltage for the first memristor switching from the initial state to a low-resistance one. The forming is currently one of the key problems in designing RRAM arrays. The RRAM structures based on HfO_x with $x = 1.8$ were shown in [7] to be forming-free. The possibility of an oxygen depletion of SiO_2 films by their treatment in hydrogen ECR plasma has not been investigated previously.

The goal of this paper is to study the atomic and electronic structure of thermal SiO_2 thin films treated in hydrogen ECR plasma, to verify this treatment as a way of obtaining nonstoichiometric oxygen-depleted $SiO_{x<2}$ films, and to ascertain whether the films obtained are suitable for use as the active medium of an RRAM cell.

2. SAMPLES AND METHODS

Stoichiometric SiO_2 films 20 nm in thickness were obtained by thermal Si (100) oxidation; KDB p^{++}–Si was taken to use the silicon substrate as the lower electrode of a MIM structure thereafter. The SiO_2 films

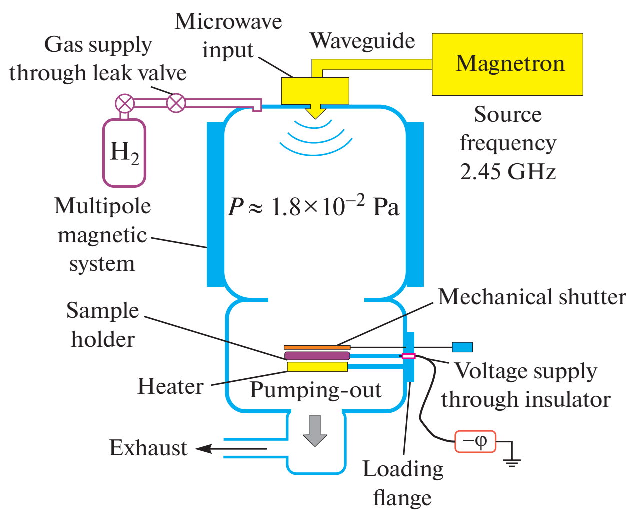

Fig. 1. Schematic view of the ECR plasma facility. The loader includes a sample holder and a shutter to control the exposure time.

were treated in a vacuum chamber assembled on the basis of an exhaust unit with a turbo-molecular pump (a residual pressure in the chamber less than 10^{-4} Pa) into which an antenna-type hydrogen ECR plasma source with a multipole magnetic system was built (Fig. 1). The operating frequency of the source is 2.45 GHz. The ECR plasma was excited at a hydrogen pressure in the vacuum chamber of 1.8×10^{-2} Pa. The power pumped into the plasma was 76 W at a magnetron current of 20 mA (the empirically established optimal value). A bias potential of -300 V was fed to the copper sample holder. The temperature of the substrate when exposed to the plasma increased by no more than 17°C. A series of SiO_2 films was obtained with various exposure times in the hydrogen ECR plasma: 2, 6, and 14 min.

To measure the current–voltage characteristics (CVCs), a layer of Ni contacts 0.2×0.2 mm^2 in size was deposited on p^{++}-Si/SiO_2 structures by electron-beam evaporation. The CVCs were measured with a Keithley 6517a electrometer at room temperature.

The X-ray photoelectron spectra (XPSs) were measured with a VG ESCALAB HP spectrometer (Great Britain) using a non-monochromatic AlK_α emission (1486.6 eV, 150 W). The full width at half maximum (FWHM) of the Au4$f_{7/2}$ line at an analyzer transmission energy of 20 eV was 1.1 eV. The samples were fixed to double-sided copper scotch tape. The method of an internal standard with the C1s line (binding energy $E_B = 284.8$ eV) was applied to calibrate the photoelectron peaks. The spectra were measured at an analyzer transmission energy of 20 eV. The O-to-Si atomic concentration ratio (parameter x) was determined from the integrated intensities of the O1s and Si2p photoelectron lines after the Shirley background subtraction by taking into account the corresponding atomic sensitivity factors (ASFs) of the elements.

~~Our~~ quantum-chemical simulations were performed within the density functional theory in the model of periodic cells in the Quantum ESPRESSO software package [8]. We used the hybrid exchange-correlation ~~parametrization~~ functional B3LYP, which provides the proper band gap of the oxides [9, 10]. The cutoff energy of plane waves was taken to be 950 eV; the core was taken into account via norm-conserving pseudo-potentials. The oxygen vacancies in SiO_2 were simulated by the removal of oxygen atoms in the α-SiO_2 supercell followed by structural relaxation. The computational technique was validated for SiO_x previously [11]. The valence band XPSs were calculated by summing the spectra of the projected density of states (PDOS) Si3s, Si3p, O2s, and O2p with weight factors of 3.061, 0.842, 0.964, and 0.128, respectively, derived from agreement between the calculation and experiment for stoichiometric SiO_2 with their smoothing by a Gaussian with $\sigma = 1.3$ eV.

3. RESULTS AND DISCUSSION

SiO_2 treatment in hydrogen ECR plasma for more than 2 min leads to a broadening of the Si2p XPS into the low-energy spectral range, the more so the longer the treatment time (Fig. 2). For the original film and the one treated for 2 min the FWHM of the peak is 1.9 eV; for the films treated for 6 and 14 min it is 2.0 and 2.05 eV, respectively. Deconvolution of the Si2p XPS into individual spectral components shows that the spectrum of the untreated film is described by a single peak with $E_B = 103.5$ eV typical of silicon in the charge state 4+ (Si^{4+}). An additional peak at $E_B = 102.5$ eV typical of Si^{3+} [12] appears when deconvolving the spectrum of the sample with 6-min treatment. The contributions of the Si^{4+} and Si^{3+} states to this spectrum are 94 and 6%, respectively. Two additional peaks at $E_B = 102.5$ eV (from Si^{3+}) and $E_B = 101.6$ eV (from Si^{2+}) [12] are observed in the decomposition of the Si2p spectrum for the SiO_2 film treated for 14 min. The contributions from Si^{4+}, Si^{3+}, and Si^{2+} to the Si2p XPS for this sample are 87, 11, and 2%, respectively.

The noticeable signal from Si^{3+} and Si^{2+} in the Si2p XPS suggests a high concentration of oxygen vacancies (Si–Si bonds) in the investigated samples. The parameter x = [O]/[Si] for the films treated in the plasma for 6 and 14 min with respect to the atomic concentrations of oxygen and silicon is estimated to be 1.9 and 1.85, respectively. For the original SiO_2 sample the ratio [O]/[Si] ≈ 2. Since the mean free paths of the photoelectrons from the Si2p (3.7 nm) and O1s (2.8 nm) levels in SiO_2 are fairly close, the influence of the adsorbates (the screening of the signal intensity from silicon and oxygen) was disregarded when determining the ratio [O]/[Si].

Thus, thermal SiO_2 treatment in hydrogen ECR plasma gives rise to a nonstoichiometric oxygen-depleted silicon oxide $SiO_{x<2}$, with x being smaller the longer the treatment time.

The atomic structure of $SiO_{x<2}$ can be described either by the random bonding (RB) model, when the Si–Si and Si–O bonds are distributed statistically randomly over the oxide structure, or by the random mixture (RM) model, when Si separates into clusters, and a combination of these models [13, 14]. According to the XPS data, there are no clusters in the plasma-treated Si films. In the RB model the atomic structure of SiO_x is described by five sorts of Si–O(ν)Si(4 – ν) tetrahedrons, where ν = 0, 1, 2, 3, 4 (the charge states of the central silicon atom Si^0, Si^{1+}, Si^{2+}, Si^{3+}, and Si^{4+}, respectively), with the fraction of tetrahedrons of a given sort in SiO_x being defined by the statistic

$$W_\nu(x) = \frac{4!}{\nu!(4-\nu)!}\left(\frac{x}{2}\right)^\nu\left(1-\frac{x}{2}\right)^{4-\nu}. \quad (1)$$

Using this formula, it is easy to calculate that 94% of the Si–O(4) tetrahedrons and 6% of Si–O(3)Si in the SiO_x structure correspond to $x \approx 1.97$ (the fraction of Si–O(ν)Si(4 – ν) tetrahedrons with ν = 2, 1, 0 for a given x is 0.131% in total. It is this ratio of Si^{4+} and Si^{3+} that was derived for the film with 6-min treatment and, hence, $x \approx 1.97$ for this film. SiO_x with $x \approx 1.94$ in the RB model consists of 88% of Si–O(4), 11% of Si–O(3)Si, and 1% of Si–O(2)Si(2) (the contribution of Si–O(1)Si(3) and Si–Si(4) is 0.01%). This ratio of the fractions of tetrahedrons is close to the estimated ratio of the contributions from Si^{4+}, Si^{3+}, and Si^{2+} to the Si2*p* XPS for the film treated in the plasma for 14 min. Thus, $x \approx 1.94$ for this film. The values of the parameter x that are given by the description of the atomic structure of the investigated SiO_x films by the RB model qualitatively agree with those derived from the experimental O1*s* and Si2*p* XFS data. The quantitative discrepancy is explained by a low accuracy of the latter method (the typical error is about 5%).

The O1*s* XPS for all our SiO_x samples has a maximum at E_B = 532.5 eV and gives almost coincident bulk plasmon energies, 22.5 ± 0.2 eV (Fig. 3). This is consistent with the weak dependence of $\hbar\omega_B$ on x for SiO_x at $1 < x < 2$ established previously [15]. Since the O1*s* XPS also reflects the spectrum of the photoelectron energy loss due to interband transitions, the oxide band gap E_g can be estimated by a linear interpolation of the edge of this spectrum to the background level (Fig. 4). In this way we obtained E_g = 8.3, 8.0, and 7.8 eV, respectively, for the original sample and the samples treated in the ECR plasma for 6 and 14 min. Despite the low accuracy of the method related to the arbitrariness in choosing the energy range for the linear interpolation, we revealed the proper trend of the dependence $E_g(x)$ for SiO_x: E_g also decreases with

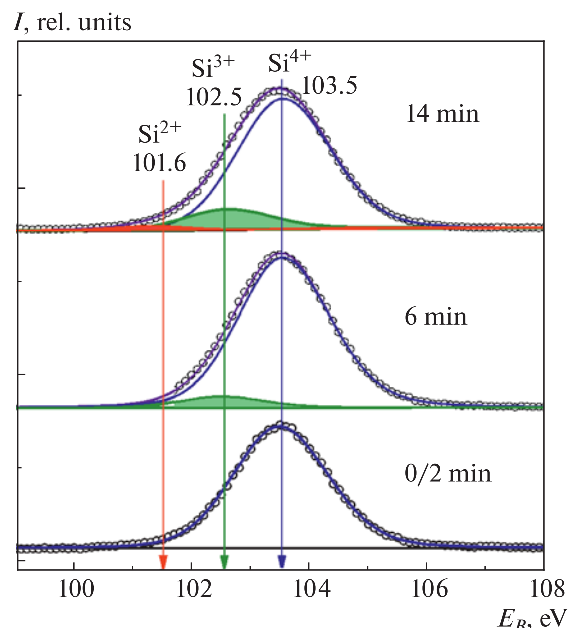

Fig. 2. Deconvolution of the Si2*p* XPS for the measured SiO_2 and SiO_x samples into individual components. The symbols represent the experiment; the blue, red, and green lines indicate the decomposition components; the violet line indicates the sum of the decomposition components. The deconvolution was performed by taking into account the asymmetry of the Si2*p* peak with an asymmetry coefficient of 8%.

decreasing x. For stoichiometric SiO_2 the derived E_g is consistent with the well-known data [16].

The valence band XPSs for the original film and the film treated in the plasma for 14 min are well described by the XPSs calculated within the density functional theory, respectively, for stoichiometric SiO_2 and SiO_2 with oxygen vacancies (Fig. 5). Both calculated and experimental spectra demonstrate a broadening of the upper edge of the valence band E_V, which is clearly seen in the corresponding difference spectra. The broadening in the calculated spectra is attributable to the defective layers in the band gap from oxygen vacancies (Si–Si bonds), with this broadening being greater the high the concentration of vacancies [11]. We can select such a concentration of oxygen vacancies in the modeled structure at which the calculated broadening (or the difference peak) will coincide with the experimental one. This gives an independent method of estimating the parameter x in SiO_x [17]. Thus, we established that the experimentally observed broadening of the valence band XPS after 14-min film treatment is well described by the calculated one when simulating one oxygen vacancy in a 32-atom supercell, corresponding to an atomic ratio [O]/[Si] ≈ 1.92.

The accuracy of this method is limited by the fairly low signal-to-noise ratio of the experimental valence

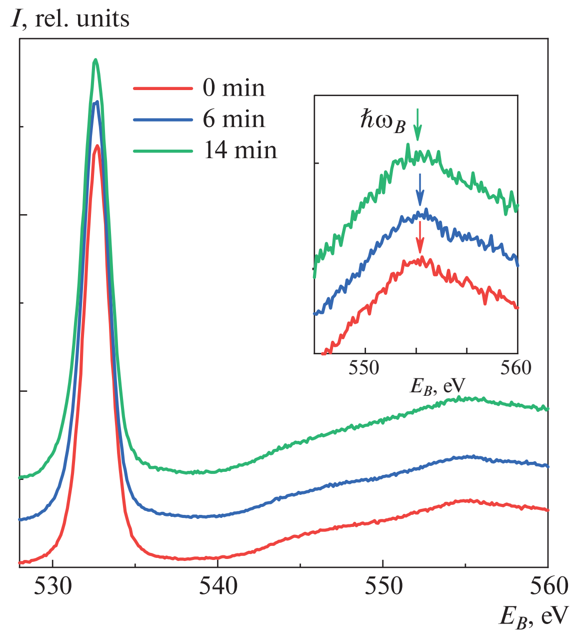

Fig. 3. O1*s* XPSs for the original SiO_2 and after its treatment in the plasma for 6 and 14 min. The inset shows the maxima of the spectra corresponding to the bulk plasmon energy.

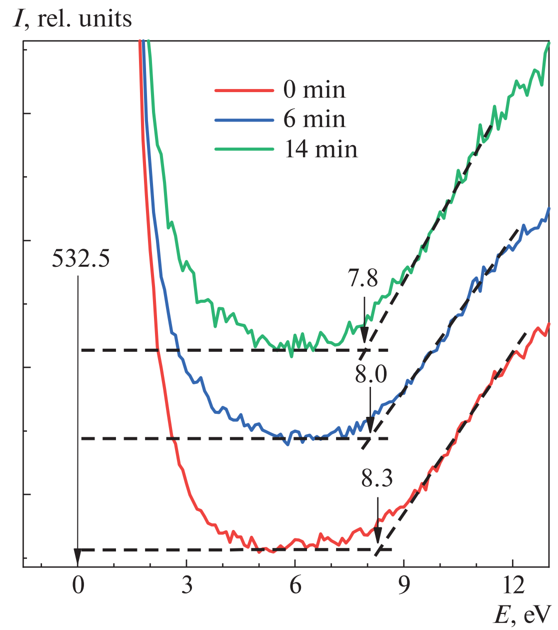

Fig. 4. Spectra of the O1*s* photoelectron energy loss and an estimate of E_g for the original SiO_2 and after its treatment in the plasma for 6 and 14 min.

band XPSs measured with the spectrometer without a monochromator. In particular, big noise (and a small deviation of x from 2) did not allow this method to be applied to estimate the parameter x in the SiO_x film treated in the plasma for 6 min. The parameter x for the film with 14-min plasma treatment derived by comparing the calculated and experimental valence band XPSs is close to its value deduced from the description of the atomic structure of this sample in the RB model, $x \approx 1.94$. This confirms the conclusion that the film structure is described by the RB model and that the method of estimating the parameter x from the ratio of the O1*s* and Si2*p* XPSs gave underestimated values.

To ascertain whether the $SiO_{x<2}$ films obtained are suitable for use as the active medium of an RRAM cell, we measured the CVCs of three p^{++}-Si/SiO_x/Ni structures in which the oxide layer was treated in the hydrogen ECR plasma for 2, 6, and 14 min (Fig. 6). It can be seen that the structures where the oxide layer was treated for more than two minutes have a typical CVC for a memristor: they are able to switch between the high (HRS) and low (LRS) resistive states in a reversible way. The memory window, i.e., the ratio of the LRS and HRS currents, increases as the treatment time of the functional layer in the plasma increases. On the CVCs of the structures with oxide layer treatment times of 2, 6, and 14 min the ratio of the LRS and HRS currents at a voltage of 2 V is 2, 10^3, and 2×10^7, respectively. A detailed study of the memristor properties of the structures obtained is the subject of further investigations.

Thus, the treatment of thermal SiO_2 thin films in the hydrogen ECR plasma gives rise to nonstoichiometric $SiO_{x<2}$ that can be used as the active medium of memristors. However, our data do not allow the degree of homogeneity of the SiO_x films obtained to be ascertained. This question remains open.

4. CONCLUSIONS

In this paper we studied the atomic and electronic structure of thermal SiO_2 thin films treated in hydrogen electron cyclotron resonance plasma for various times. An analysis of the X-ray photoelectron spectra showed that such treatment leads to an oxygen depletion of thermal SiO_2, with the degree of depletion being higher the longer the treatment time. We established that the atomic structure of the nonstoichiometric $SiO_{x<2}$ films obtained by plasma treatment is described by the random bonding model, in which the Si–Si and Si–O bonds are distributed statistically randomly over the oxide structure. We estimated the parameter x by three different methods: from the integrated intensity of the O2*s* and Si2*p* XPSs; from the deconvolution of the Si2*p* XPS into individual components and the description in the RB model; from a comparison of the experimental valence band XPSs and those calculated from first principles. The band gap was estimated by analyzing the spectra of the O1*s* photoelectron energy loss; 8.3, 8.0, and 7.8 eV were obtained, respectively, for the original sample and the samples treated in the plasma for 6 and 14 min. We established that the CVCs of the p^{++}-Si/SiO_x/Ni

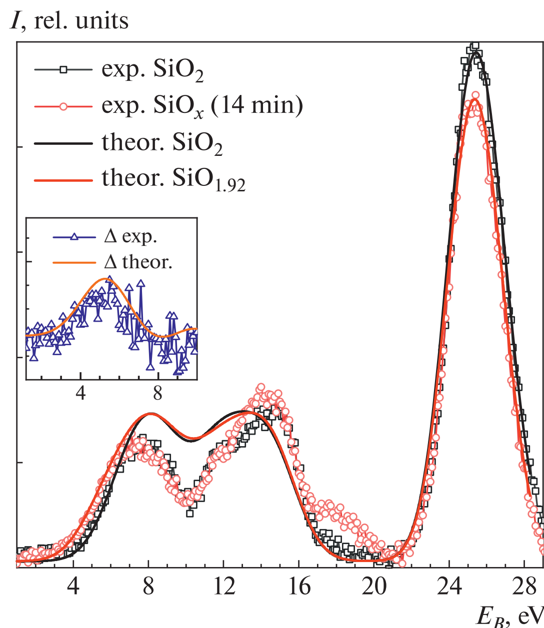

Fig. 5. Experimental (symbols) valence band XPSs and those calculated from first principles (lines) for SiO_2 and SiO_x. The inset shows the corresponding difference spectra.

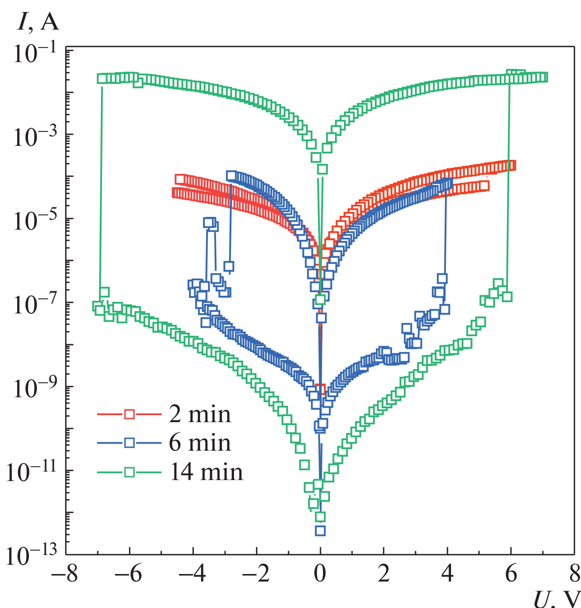

Fig. 6. CVCs of p^{++}-Si/SiO_x/Ni structures with various treatment times of the functional layer in the hydrogen plasma.

structures where the oxide layer was treated in the hydrogen ECR plasma have a typical CVC for a memristor. In this case, the memory window of the memristors increases with exposure time in the hydrogen plasma. Thus, the treatment of stoichiometric thermal SiO_2 in hydrogen ECR plasma is an efficient method of obtaining nonstoichiometric $SiO_{x<2}$ films suitable for use as the active medium of an RRAM cell.

FUNDING

This work was supported by the Russian Science Foundation (project no. 19-19-00286). The simulations were performed at the computational cluster of the Data Processing Center of the Novosibirsk State University.

REFERENCES

1. F. Zhou, L. Guckert, Y. F. Chang, E. E. Swartzlander, and J. Lee, Appl. Phys. Lett. **107**, 183501 (2015).
2. A. Mehonic, A. L. Shluger, D. Gao, I. Valov, E. Miranda, D. Ielmini, A. Bricalli, E. Ambrosi, C. Li, J. J. Yang, Q. F. Xia, and A. J. Kenyon, Adv. Mater. **30**, 1801187 (2018).
3. D. S. Jeong, R. Thomas, R. S. Katiyar, J. F. Scott, H. Kohlstedt, A. Petraru, and C. S. Hwang, Rep. Progr. Phys. **75**, 076502 (2012).
4. A. A. Chernov, D. R. Islamov, A. A. Pik'nik, T. V. Perevalov, and V. A. Gritsenko, ECS Trans. **75**, 95 (2017).
5. V. Sh. Aliev, V. N. Votentsev, A. K. Gutakovskii, S. M. Maroshina, and D. V. Shcheglov, J. Surf. Invest.: X-ray, Synchrotron Neutron Tech. **1**, 454 (2007).
6. Y. Y. Chen, L. Goux, J. Swerts, M. Toeller, C. Adelmann, J. Kittl, M. Jurczak, G. Groeseneken, and D. J. Wouters, IEEE Electron. Dev. Lett. **33**, 483 (2012).
7. V. S. Aliev, A. K. Gerasimova, V. N. Kruchinin, V. A. Gritsenko, I. P. Prosvirin, and I. A. Badmaeva, Mater. Res. Express **3**, 085008 (2016).
8. P. Giannozzi, O. Andreussi, T. Brumme, et al., J. Phys.: Condens. Matter **29**, 465901 (2017).
9. V. A. Gritsenko, T. V. Perevalov, V. A. Volodin, V. N. Kruchinin, A. K. Gerasimova, and I. P. Prosvirin, JETP Lett. **108**, 226 (2018).
10. D. R. Islamov, V. A. Gritsenko, T. V. Perevalov, O. M. Orlov, and G. Y. Krasnikov, Appl. Phys. Lett. **109**, 052901 (2016).
11. T. V. Perevalov, V. A. Volodin, Yu. N. Novikov, G. N. Kamaev, V. A. Gritsenko, and I. P. Prosvirin, Phys. Solid State **61**, 2560 (2019).
12. A. Barranco, J. A. Mejias, J. P. Espinos, A. Caballero, A. R. Gonzalez-Elipe, and F. Yubero, J. Vac. Sci. Technol. A **19**, 136 (2001).
13. H. R. Philipp, J. Noncryst. Sol. 8–10, 627 (1972).
14. Y. N. Novikov and V. A. Gritsenko, J. Appl. Phys. **110**, 014107 (2011).
15. F. G. Bell and L. Ley, Phys. Rev. B **37**, 8383 (1988).
16. K. A. Nasyrov, S. S. Shaimeev, V. A. Gritsenko, and J. H. Han, J. Appl. Phys. **105**, 123709 (2009).
17. T. V. Perevalov, V. A. Gritsenko, D. R. Islamov, and I. P. Prosvirin, JETP Lett. **107**, 55 (2018).

Translated by V. Astakhov

SPELL: 1. memristor